References and Notes

(1) R. W. Taft, Jr., in "Steric Effects in Organic Chemistry", M. S. Newman, Ed., Wiley, New York, N.Y., 1957, p 556.
(2) R. W. Taft, Jr., *J. Am. Chem. Soc.*, **74**, 2729, 3120 (1952).
(3) C. K. Ingold, *J. Chem. Soc.*, 1032 (1932).
(4) D. R. Storm and D. E. Koshland, Jr., *J. Am. Chem. Soc.*, **94**, 5805 (1972).
(5) (a) M. Charton, *J. Am. Chem. Soc.*, **91**, 615 (1969); **97**, 1552 (1975); (b) W. A. Nugent and J. K. Kochi, *ibid.*, **98**, 273 (1976).
(6) (a) D. F. DeTar and C. J. Tenpas, *J. Am. Chem. Soc.*, **98**, 4567 (1976); (b) *J. Org. Chem.*, **41**, 2009 (1976).
(7) W. T. Wipke and P. Gund, *J. Am. Chem. Soc.*, **96**, 299 (1974).
(8) E. M. Engler, J. D. Andose, and P. v. R. Schleyer, *J. Am. Chem. Soc.*, **95**, 8005 (1973).
(9) F. Becker, *Z. Naturforsch. B*, **16**, 236 (1961).
(10) N. L. Allinger, M. T. Tribble, M. A. Miller, and D. H. Wertz, *J. Am. Chem. Soc.*, **93**, 1637 (1971).
(11) A. J. Gordon and R. A. Ford, "The Chemist's Companion", Wiley, New York, N.Y., 1972, p 107.
(12) C. Fry, E. M. Engler, and P. v. R. Schleyer, *J. Am. Chem. Soc.*, **94**, 4628 (1972); J. Slutsky, R. C. Bingham, P. v. R. Schleyer, W. C. Dicksson, and H. C. Brown, *ibid.*, **96**, 1969 (1974).
(13) D. F. DeTar, *J. Am. Chem. Soc.*, **96**, 1255 (1974).
(14) N. L. Allinger and G. A. Lane, *J. Am. Chem. Soc.*, **96**, 2937 (1974).
(15) N. B. Chapman, J. Shorter, and K. J. Toyne, *J. Chem. Soc.*, 2543 (1961).
(16) N. L. Allinger and L. A. Freiberg, *J. Am. Chem. Soc.*, **84**, 2836 (1962).
(17) N. L. Allinger and S-E. Hu, *J. Org. Chem.*, **27**, 3417 (1962).
(18) S. Winstein and N. J. Holness, *J. Am. Chem. Soc.*, **77**, 5562 (1955).
(19) D. R. Stull, E. F. Westrum, Jr., and G. C. Sinke, "The Chemical Thermodynamics of Organic Compounds", Wiley, New York, N.Y., 1969.
(20) N. L. Allinger and J. L. Coke, *J. Org. Chem.*, **26**, 2096 (1961).
(21) W. G. Dauben, O. Rohr, A. Labbanf, and F. D. Rossini, *J. Phys. Chem.*, **64**, 283 (1960).
(22) W. P. Campbell and D. Todd, *J. Am. Chem. Soc.*, **64**, 928 (1942).
(23) J. E. Anderson and H. Pearson, *J. Chem. Soc., Perkin Trans. 2*, 1779 (1974).
(24) M. J. Barrow, M. Currie, K. M. Muir, J. C. Speakman, and D. N. J. White, *J. Chem. Soc., Perkin Trans. 2*, 15 (1975).
(25) D. F. DeTar, "Computer Programs for Chemistry", Vol. 4, D. F. DeTar, Ed., Academic Press, New York, N.Y., 1972, p 71.

Generalized Valence Bond Description of the Low-Lying States of NiCO[1]

Stephen P. Walch and W. A. Goddard III*[2]

Contribution No. 5303 from the Arthur Amos Noyes Laboratory of Chemical Physics, California Institute of Technology, Pasadena, California 91125.

Received April 5, 1976

Abstract: GVB and GVB-CI wave functions (using a double ζ basis) have been obtained as a function of internuclear distance for the lowest three states of NiCO. The wave functions lead to a qualitative description in which the Ni atom is neutral with a $(4s)^1(3d)^9$ atomic configuration. The CO lone pair delocalizes slightly onto the Ni leading to the 4s-like orbital hybridizing away from the CO. The dπ pairs on the Ni are slightly back-bounding to the CO. The three bound states are $^3\Sigma^+$, $^3\Pi$, and $^3\Delta$ consisting of the singly occupied 4s-like orbital plus a single d hole in a σ, π, or δ orbital, respectively. The ground state is found to be $^3\Delta$ with calculated R_e = 1.90 Å, D_e = 1.15 eV = 26.5 kcal/mol, and ω_e(Ni-C) = 428 cm^{-1}, all reasonable values, although direct information on NiCO is not yet available. The adiabatic excitation energies are calculated as 0.240 eV to $^3\Sigma^+$ and 0.293 eV to $^3\Pi$. The states with $(4s)^2(3d)^8$ configurations on the Ni lead to repulsive potential curves with vertical excitation energies in the range of 3.0 to 5.0 eV.

I. Introduction

The study of the reactions occurring at metal surfaces constitutes an important field of modern chemical research. As one step in a program directed toward understanding one such reaction, the methanation of CO on a nickel surface, we are investigating the bonding of CO to the surface. As the first step of examining the bonding of CO to a Ni surface, we have carried out extensive studies of the bonding of CO to a single Ni atom. These results will be useful in understanding how to study the bonding of CO to larger complexes and indeed already provide some useful insights into the nature of the bond to the surface.

In addition, matrix isolation experiments have provided evidence for the existence of $Ni(CO)_n$, n = 1-4.[3] It is expected that the results of the NiCO calculations will suggest some experimental tests for these model systems.

In section II we describe basic concepts of the GVB wave functions, the effective potential, and the basis set used. In section III the results obtained are discussed in qualitative terms, while section IV examines in more detail some of these concepts in terms of the GVB wave function. Section V discusses the excited states. In section VI we describe the CI calculations. Section VII compares results with the ab initio effective potential (AIEP) and the modified effective potential (MEP) used here.

II. The Wave Functions

A. The GVB Method. The details of the GVB method have been described elsewhere.[4] The GVB wave function can be viewed as a normal closed-shell Hartree-Fock (HF) wave function,

$$\mathcal{A}(\phi_1\phi_1\alpha\beta\phi_2\phi_2\alpha\beta\ldots)$$

in which certain doubly occupied singlet pairs

$$\phi_i\phi_i\alpha\beta \tag{1}$$

are replaced by GVB pairs

$$(\phi_{ia}\phi_{ib} + \phi_{ib}\phi_{ia})\alpha\beta = (\lambda_1\phi_{i1}^2 - \lambda_2\phi_{i2}^2)\alpha\beta \tag{2}$$

where each electron of the pair is allowed to have its own GVB orbital ϕ_{ia} or ϕ_{ib}, the overlap of which,

$$S_{ab}^{\,i} = \langle\phi_{ia}|\phi_{ib}\rangle \tag{3}$$

is in general nonzero. In the perfect pairing approximation to GVB (referred to as GVB-PP), the GVB orbitals of a given pair are taken as orthogonal to those of all other pairs (strong orthogonality restriction) and in addition the spin eignfunction is restricted to the form where the maximum number of pairs are singlet coupled (perfect pairing restriction). For nonsinglet states we also allow n high coupled orbitals.

$$\phi_1 \ldots \phi_n \alpha\alpha \ldots \alpha \qquad (4)$$

To simplify the variational equations, the nonorthogonal orbitals $\{\phi_{ia},\phi_{ib}\}$ are expanded in an orthonormal set $\{\phi_{i1},\phi_{i2}\}$ (referred to as the natural orbitals) as in (2).

B. The Modified Effective Potential. In order to carry out calculations of the type described here at reasonable cost, it is expedient to use an effective potential to replace the 18-electron Ar core of the transition metal. Considerable progress in this area has been made by Melius, Olafson, and Goddard[5] in developing an effective potential for Ni which allows near ab initio accuracy, referred to as the ab initio effective potential (AIEP). However, for the Ni atom ab initio calculations themselves lead to incorrect separations of the states if carried out with the usual basis and level of correlation. For example, using the Wachter basis[9], the $s^1d^9(^3D)$ state is calculated in the Hartree-Fock (HF) description to be 2.32 eV above the $s^2d^8(^3F)$ state, whereas the experimental separation is only 0.03 eV.[6,7] There are three contributions to this error: (1) basis set—the s^1d^9 state requires more diffuse d functions than the s^2d^8 state for which the basis was optimized; (2) correlation effects involving s, p, and d basis functions; and (3) correlation effects involving f functions. Including effects 1 and 2 (highly correlated wave functions using an extended basis with tight p functions) leads to a decrease in the excitation energy from 2.32 to 0.22 eV,[21] with the remaining 0.25 eV error presumably due to f functions. The level of correlation required here is impractical for molecular systems with transition metals, and we have adopted an alternative procedure for including these effects in an approximate way.

Sollenberger, Goddard, and Melius[8] have found that these missing efforts in the atoms can be imitated by adding additional terms to the ab initio effective potential in such a way as to reproduce the correct atomic separations and orbital shapes. Thus it was anticipated that the bond lengths and geometries resulting from interaction with other atoms would be accurate. Indeed this procedure does lead to reasonable bond lengths and bond energies for NiH and FeH.[8] The resulting potential referred to as the modified effective potential (MEP) was used for the calculations described here. Some comparisons with the results of the AIEP are made in section VII.

C. Basis Set and Geometry. The basis for Ni was selected from the set optimized for the ground states of the third-row atoms by Wachters.[9] We have used all five d primitives (of each type) but, as discussed in ref 5, only the outer four s-functions are needed for describing the coreless Hartree-Fock orbital. The inner four d primitives were contracted together and the inner two s functions were contracted together with the relative coefficients based on Hartree-Fock calculations for the $s^2d^8(^3F)$ state of the Ni atom (ref 8). In addition, a single p primitive with $\alpha = 0.12$ was added in each direction (to allow polarization effects involving the 4s orbital). The final basis for Ni (see Table I) is identical with that in ref 8 except for the p functions and slight differences in the s functions.

The basis for carbon and oxygen is the Dunning (3s2p) contraction[10] of the Huzinaga (9s,5p) basis. This contraction is double ζ valence but uses a single 1s-like contracted function and leads to energies which are generally within 0.0001 hartree of those obtained with the "double ζ" contraction.[11]

We have taken the CO bond distance as 2.17 bohr which is close to the experimental CO bond distance in $Ni(CO)_4$.[12] The NiC bond length was varied over the range of 3.2 to 3.8 bohr (the NiC distance is 3.48 bohr in $Ni(CO)_4$).[12]

III. Qualitative Description of NiCO

For the moment we will view the CO molecule as

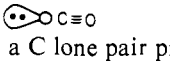

that is, a triple bond with a C lone pair protruding from the carbon.

Table I. The Nickel Basis Set[a]

	α	C
d	48.940 30	0.032 958 4
	13.716 90	0.177 800 2
	4.639 51	0.443 562 6
	1.574 33	0.565 603 9
s	0.486 41	1.000
	2.400 00	0.132 666 1
	0.940 00	0.884 440 4
	0.150 00	1.000
	0.049 00	1.000
p	0.120 00	1.000

[a] The Ni basis was taken from earlier calculations on NiH (C. Melius, unpublished work). In these calculations we have not excluded the s-like $(x^2 + y^2 + z^2)$ combinations of the d basis functions. Including these additional s functions in combination with the other s functions, which are slightly different from those used in ref 8, leads to atomic energies of −40.495 31 hartree for $^3D(s^1d^9)$ and −40.490 65 hartree for $^3F(s^2d^8)$ which are 0.0010 hartree lower and 0.0028 hartree higher, respectively, than with the basis used in ref 8.

The lowest state of the Ni atom is the $^3F_4$ state arising from the $(4s)^2(3d)^8$ configuration; however, the $^3D_3$ state arising from the $(4s)^1(3d)^9$ configuration is only 0.025 eV higher. Since spin-orbit coupling effects are not included, we will henceforth average together the various J states corresponding to a particular L and S. In this case we find that the ground state is $^3D(s^1d^9)$ with the $^3F(s^2d^8)$ state at 0.03 eV, the $^1D(s^1d^9)$ state at 0.33 eV, and the $^3P(s^2d^8)$ state at 1.86 eV.

Upon bringing the Ni and CO together we find that the s^1d^9 states are stabilized significantly with respect to the s^2d^8 states. As a result the three bound states of NiCO are all of s^1d^9 character on the Ni. Given the s^1d^9 configuration of Ni, we obtain three triplet states of NiCO, $^3\Sigma^+$, $^3\Pi$, and $^3\Delta$, depending upon whether we take the single d hole as σ, π, or δ in symmetry.

The orbitals of the $^3\Sigma^+$ state are shown in Figure 1 while the corresponding orbitals of Ni and CO are shown in Figures 2 and 3, respectively. From the orbitals one sees that (1) the 4s-like orbital hybridizes away from the CO, (2) the CO lone pair delocalizes (bonds) just slightly onto the Ni, (3) the Ni $d\pi$ orbitals delocalize slightly (back bond) into the π system of the CO, and (4) the CO π bonds are modified slightly by the Ni. For comparison, selected orbitals of the $^3\Pi$ and $^3\Delta$ states are shown in Figures 4 and 5.

The Mulliken populations (Table II) for the $^3\Sigma^+$ state reflect the above trends, the σ donation showing up in a decreased s + p_z population on carbon of 0.08 with an increase in the 4s + 4pσ + 3dσ population on the Ni of 0.09. In the π system, back-donation is reflected in an increase of 0.12 in the carbon pπ population and a corresponding decrease of 0.08 in the nickel 3dπ population.

Since the $^3\Sigma^+$ state has a dσ hole, while the $^3\Pi$ and $^3\Delta$ states have doubly-occupied dσ orbitals, one would expect the $^3\Sigma^+$ state to act as a better σ acceptor for the CO lone pairs, stabilizing the $^3\Sigma^+$ state. Since the $^3\Sigma^+$ and $^3\Delta$ states each have two doubly occupied dπ pairs, whereas the $^3\Pi$ state has only three electrons in dπ orbitals, the $^3\Sigma^+$ and $^3\Delta$ states are expected to obtain more π back-bonding than the $^3\Pi$ state. Putting these effects together would lead to the ordering

$$^3\Sigma^+ < {}^3\Delta < {}^3\Pi$$

with perhaps comparable spacings. In fact, we find that the actual ordering of states is $^3\Delta < {}^3\Sigma^+ < {}^3\Pi$ with the $^3\Delta$ and $^3\Sigma^+$

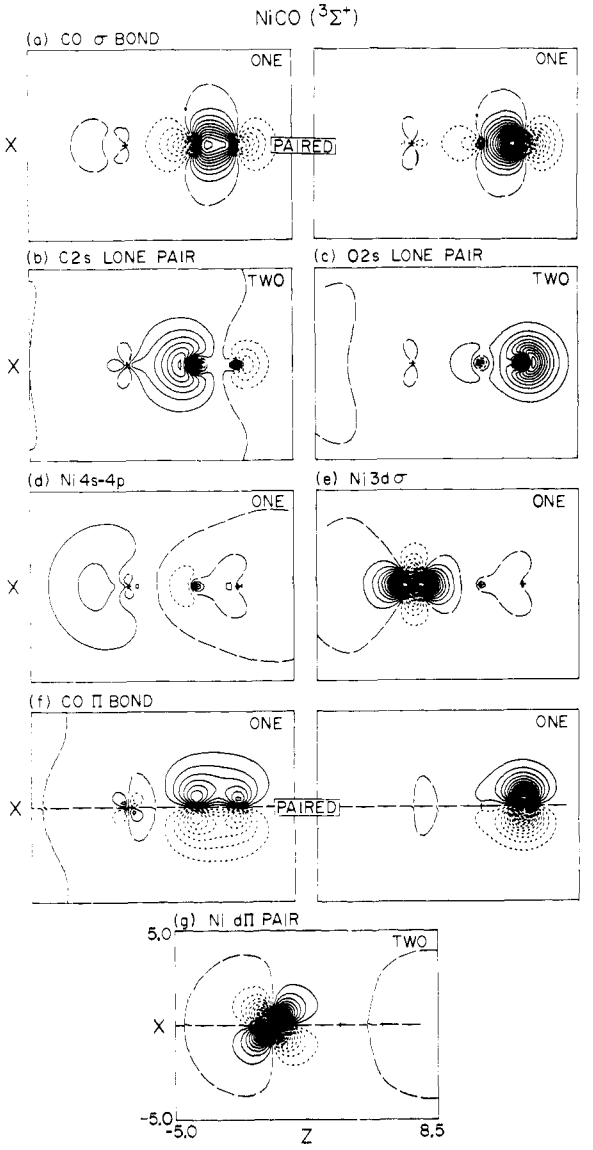

Figure 1. The GVB(3) orbitals of the $^3\Sigma^+$ state of NiCO. Unless otherwise noted, all plots have uniformly spaced contours with increments of 0.05 au. Nodal lines are indicated by long dashes. The same conventions are used for other figures unless otherwise stated.

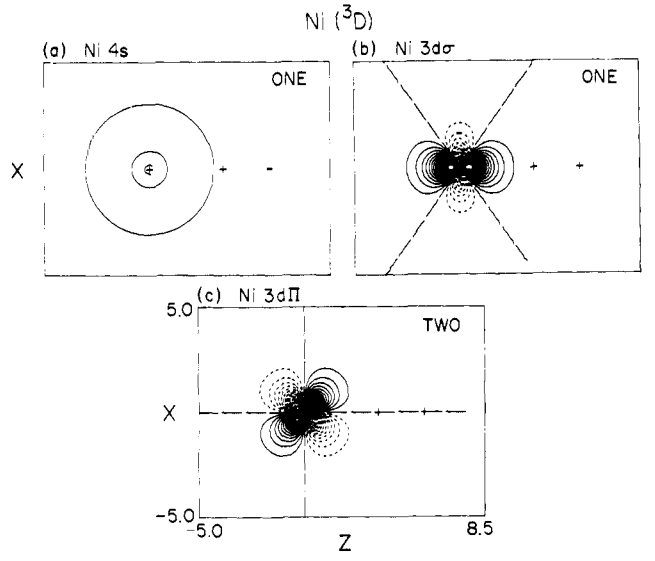

Figure 2. Selected HF orbitals of the ^{3}D state of Ni.

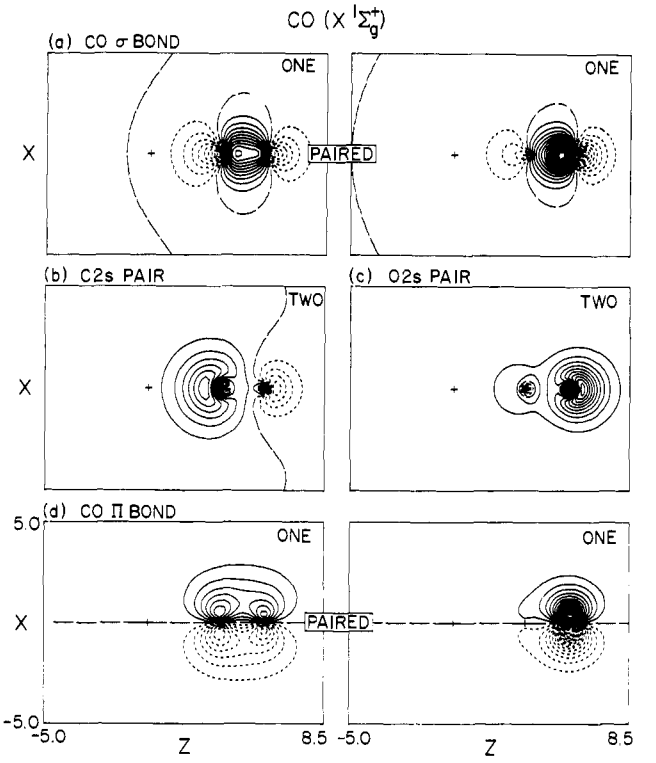

Figure 3. Selected orbitals of the GVB(3) {COσ, π_x, π_y} wave function of the X $^1\Sigma_g^+$ state of CO.

Table II. Mulliken Populations for CO and NiCO[a]

			NiCO		
		Ni(s^1d^9) + CO	$^3\Sigma^+$	$^3\Pi$	$^3\Delta$
C	s	3.8449	3.6472	3.6448	3.636 0
	p_z	0.9875	1.1001	1.0887	1.078 6
	p_x	0.5280	0.5942	0.5843	0.595 5
	p_y	0.5281	0.5942	0.5984	0.595 5
O	s	3.7846	3.8086	3.8091	3.807 4
	p_z	1.3830	1.3515	1.3519	1.350 7
	p_x	1.4720	1.4451	1.4254	1.444 4
	p_y	1.4719	1.4451	1.4491	1.444 4
Ni	4s	1.0	0.9541	1.0327	1.077 4
	4pσ	0.0	0.2376	0.2525	0.258 1
	3dσ	1.0 or 2.0	0.9009	1.8205	1.791 8
	3dπ_x	1.0 or 2.0	1.9600	0.9902	1.958 8
	4pπ_x	0.0	0.0006	0.0001	0.001 3
	3dπ_y	2.0	1.9600	1.9507	1.958 8
	4pπ_y	0.0	0.0006	0.0017	0.001 3
	δ_{xy}	1.0 or 2.0	2.0000	2.0000	1.000 0
	$\delta_{x^2-y^2}$	1.0 or 2.0	2.0000	2.0000	2.000 0
	s + p_z	4.8324	4.7473	4.7335	4.714 6
	s + p_z	5.1676	5.1601	5.1610	5.158 1
	4s + 4pσ + 3dσ	2.0 or 3.0	2.0926	3.1057	3.127 3
Totals	Ni	10.0	10.0141	10.0484	10.047 7
	C	5.8885	5.9356	5.9162	5.905 6
	O	8.1115	8.0503	8.0355	8.046 7

[a] Based on GVB wave functions at R = 1.84 Å.

states separated by 0.240 eV, whereas the $^3\Sigma^+$ and $^3\Pi$ states are separated by 0.053 eV.

Following the analysis of Melius and Goddard[17] (for NiH and Ni_2), we believe that there is one additional intraatomic effect (intraatomic coupling) favoring $^3\Delta$ and $^3\Pi$. As discussed in section IV.C, rehybridizing the 4s and 3d orbitals of the s^1d^9

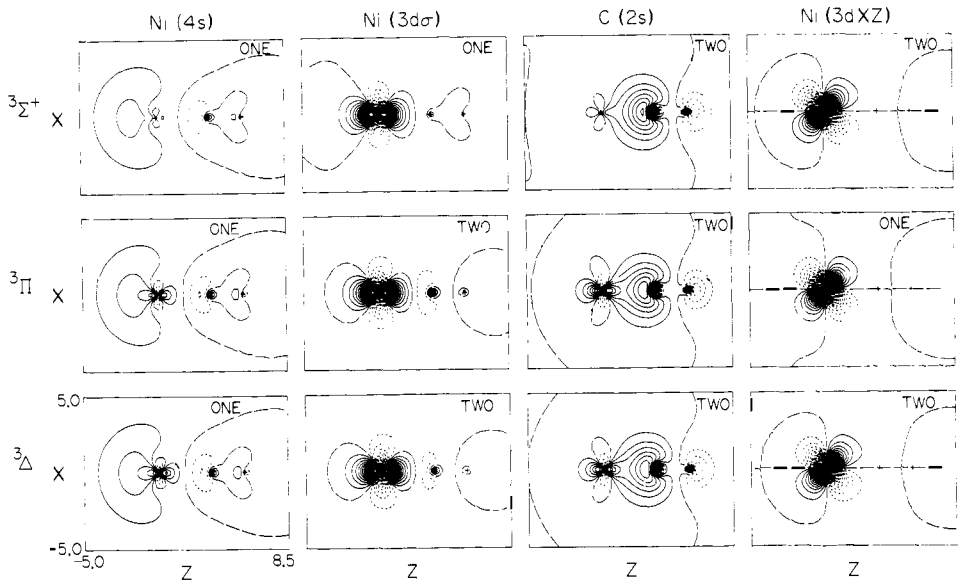

Figure 4. A comparison of selected orbitals of the GVB wave function for the $^3\Sigma^+$, $^3\Pi$, $^3\Delta$ states of NiCO.

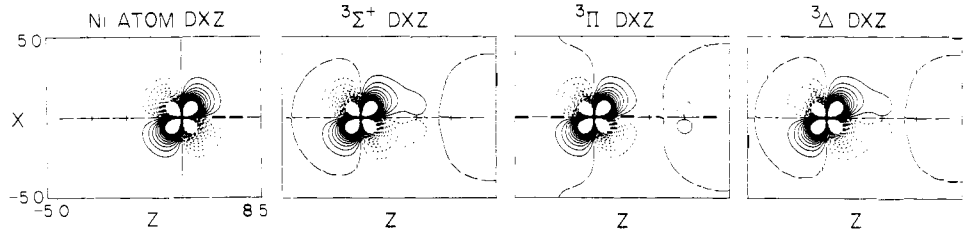

Figure 5. A comparison of the $3d_{xz}$ orbitals of Ni(^{3}D) and the $^3\Sigma^+$, $^3\Pi$, and $^3\Delta$ states of NiCO using a contour interval of 0.025 to emphasize the differences in the amount of back-bonding.

state leads to incorporation of specific components of the s^2d^8 state. However, the energies of these components differ markedly (a range of ~4 eV) depending upon the specific configuration involved. The result is that the state with the δ hole is stabilized with respect to the state of the π hole which is in turn stabilized with respect to the state with a σ hole. As a result, the $^3\Delta$ state allows greater rehybridization of the σ orbitals than the $^3\Pi$ state, and the $^3\Pi$ state allows much greater rehydridization than the $^3\Sigma$ as is clear from Figures 1 and 4.

The fact that greater rehybridization of the 4s 3d orbitals is favored for the $^3\Pi$ and $^3\Delta$ states whereas the $^3\Sigma$ state is more favorable for a pure s^1d^9 configuration results in similar σ donations (CO to Ni) for all three states (see Table II), a result that would not be expected if the intraatomic coupling were not present. As expected, the singly occupied Ni($3d\pi$) orbital of the $^3\Pi$ state leads to very little back-bonding (Ni $3d\pi_x$ Mulliken population = 0.99 as compared with 1.96 for the $3d\pi$ orbitals of the $^3\Sigma$ and $^3\Delta$ states) so that the total π back-bonding in the $^3\Pi$ state is significantly less than for the $^3\Sigma$ and $^3\Delta$ states. (See also Figure 5.)

As discussed in section V, there are low-lying $^3\Delta$ and $^3\Pi$ states arising from s^2d^8 configurations on the Ni but no comparable $^3\Sigma^+$ state. Thus in the CI the $^3\Delta$ and $^3\Pi$ states are further stabilized relative to the $^3\Sigma^+$ state, leading to the calculated spacings.

The $^3\Sigma^+$, $^3\Pi$, and $^3\Delta$ states all lead to minima at about the same R_e. For the $^3\Delta$ ground state the calculated R_e (1.90 Å) and D_e (1.15 eV) compare reasonably well with the NiC distance (1.84 Å) and average bond energy (1.53 eV) in $Ni(CO)_4$.[13] The NiC stretching constant calculated for NiCO is 428 cm^{-1} which is in the range observed for $Ni(CO)_4$ (423 cm^{-1})[13] and tentatively assigned to $Ni(CO)_3$ (457 cm^{-1})[13] and $Ni(CO)_2$ (516 cm^{-1}).[13]

IV. More Detailed Discussion of the GVB Wave Function

A. The CO Molecule. Omitting the C(2s) and O(2s) pairs and adopting a familiar notation, the ground states of $C(s^2p^2)$ and $O(s^2p^4)$ are represented as[4]

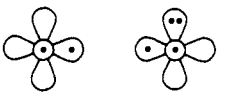

(5)

where p orbitals in the plane are represented by  and p orbitals perpendicular to the plane by ○. Coupling these so as to form a σ bond leads to two degenerate structures,

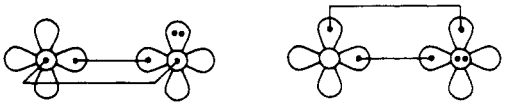

(6)

where the lines indicate bond (singlet coupled) pairs.

Considering for the moment only one of the structures (6), there is an important angular correlation of the C(2s) pair in the direction of the empty $2p\pi$ orbital (just as for the ground state of the carbon atom[4]). This leads to the description for CO,

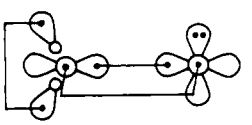

(7)

which we will refer to as GVB(3) {C(2s), σ, π_x}, to indicate which pairs are being correlated.

This single structure provides a useful description in situations where the symmetry is lowered due to bond formation. For example, (7) leads to a facile understanding of the structure of the formyl radical and of formaldehyde.[14]

One should keep in mind, however, that (7) does not exhibit the correct rotational symmetry. The correct symmetry is obtained by taking the sum of the two structures (6), and the resulting wave function is lower in energy than either of the individual structures (6). In the GVB method, this wave function may be described in an average sense by simultaneously correlating the σ, π_x, and π_y pairs in such a way that the two π directions are equivalent.[15] This wave function is referred to as GVB(3) $\{\sigma, \pi_x, \pi_y\}$ and leads to an energy 0.413 eV lower than the wave function (7). (This is essentially the triple bond picture of CO we adopted in section III.) The self-consistent orbitals of the GVB(3) $\{\sigma, \pi_x, \pi_y\}$ wave function are those shown in Figure 3.

B. NiCO. Now consider bringing up a transition metal atom to the CO molecule in a linear arrangement. Given the empty C(2p) orbital in (6), a doubly occupied $3d\pi$ orbital would be expected to delocalize onto carbon leading to resonance structures (8) which are analogous to (6)

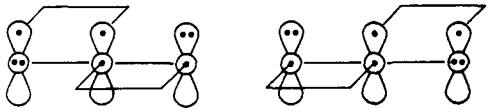

(8)

[Note here that $d\pi$ orbitals are schematically indicated in the same way as $p\pi$ orbitals, in order to keep the diagrams simple.] The delocalization of the metal $3d\pi$ orbital is expected to be more favorable if it is balanced by delocalization of the C(2s) orbital into empty metal σ orbitals, thus leading to less net transfer of charge. Thus the valence bond description leads naturally to the concept of CO as a σ donor and π acceptor in bonding to a transition metal.

As with CO the orbitals of NiCO were solved for with a three-pair wave function, GVB(3) $\{\sigma, \pi_x, \pi_y\}$, in which the π directions are kept equivalent. This wave function may be thought of as a superposition of the structures (8) in the same way that the analogous wave function for CO was described as a superposition of the structures (6).

C. The Intraatomic Coupling Effect.[17] Consider the wave function for the $^3\Delta$ state of NiCO

$$\psi(s^1d^9) = \mathcal{A}\{[\text{CORE}](3d\sigma)^2(4s)(3d\delta)\alpha\beta\alpha\alpha\} \quad (9)$$

where most orbitals (including the bonds) have been collected into [CORE]. In the GVB wave function all orbitals are solved for self-consistently; however, for the time being we restrict the 4s and $3d\sigma$ orbitals to mix only with each other (rehybridize). The result is

$$\mathcal{A}\{[\text{CORE}](3d\sigma - \lambda 4s)^2(4s + \lambda 3d\sigma)(3d\delta)\alpha\beta\alpha\alpha\} = \psi(s^1d^9) + \lambda\psi(s^2d^8) \quad (10)$$

where

$$\psi(s^2d^8) = \mathcal{A}\{[\text{CORE}](4s)^2(3d\sigma)(3d\delta)\alpha\beta\alpha\alpha\} \quad (11)$$

and where we neglected terms of order λ^2 (for the self-consistent wave function, λ is $\sim$0.21). Thus rehybridizing the orbitals leads to mixing of s^2d^8 character into the wave function.

The component of s^2d^8 character in (10) has ^{3}F symmetry; however, in the $^3\Pi$ state the term corresponding to (11) is[18]

$$\mathcal{A}\{[\text{CORE}](4s)^2(3d\sigma)(3d\pi)\alpha\beta\alpha\alpha\} \quad (12)$$

Assuming a triplet d^2 state (following the holes of d^8) with $M_S = 1$, the ^{3}F and ^{3}P states with $M_L = 1$ are described as

$$|L = 3, M_L = 1\rangle = \sqrt{\frac{4}{10}}\,|m_1 = 1, m_2 = 0\rangle + \sqrt{\frac{6}{10}}\,|m_1 = 2, m_2 = -1\rangle$$

$$|L = 1, M_L = 1\rangle = \sqrt{\frac{6}{10}}\,|m_1 = 1, m_2 = 0\rangle - \sqrt{\frac{4}{10}}\,|m_1 = 1, m_2 = -1\rangle \quad (13)$$

so that

$$|m_1 = 1, m_2 = 0\rangle = \sqrt{\frac{4}{10}}\,|L = 3, M_L = 1\rangle + \sqrt{\frac{6}{10}}\,|L = 1, M_L = 1\rangle \quad (14)$$

Thus the configuration in (12) is 40% ^{3}F and 60% ^{3}P corresponding to an atomic excitation energy of 1.13 eV. As a result, rehybridization should be less important for the $^3\pi$ state than for the $^3\Delta$ state. In the $^3\Sigma$ state the s^1d^9 wave function is[19]

$$\mathcal{A}\{[\text{CORE}](3d\sigma)(4s)\alpha\alpha\} \quad (15)$$

and hence *no* rehybridization is allowed (in this approximation). These expectations are borne out by the shapes of the orbitals as indicated in Figures 1 and 4.

V. The s^2d^8 Excited States

The three bound states of NiCO all arise from the $^3D(s^1d^9)$ state of the Ni atom. Higher states are derived from the ^{3}F- and $^3P(s^2d^8)$ states of Ni. Given two holes in the d shell and classifying the *atomic states* according to their rotational symmetry relative to the molecular axis leads to five different triplet states depending on how the two holes are distributed over the d orbitals. Taking $\delta\pi$ or $\delta\sigma$ holes leads to a pure ^{3}F state which is only 0.03 eV higher than the ^{3}D state. Taking $\pi\pi$ holes leads to 80% ^{3}F and 20% ^{3}P with an excitation energy of 0.40 eV, taking $\sigma\pi$ holes leads to 40% ^{3}F and 60% ^{3}P corresponding to an excitation energy of 1.13 eV, and taking $\delta\delta$ holes leads to 20% ^{3}F and 80% ^{3}P leading to an excitation energy of 1.49 eV.[16] Thus, based only on the atomic states involved, one would expect the ordering

$$\delta\pi \cong \delta\sigma < \pi\pi < \sigma\pi < \delta\delta$$

Upon bringing up a CO, the above ordering would be modified depending on the favorability for the atomic configuration to function as a σ acceptor, π donor. On this basis one would expect the state with the $\delta\sigma$ holes to be stabilized relative to the state with the $\delta\pi$ holes. Similarly, one might expect the state with the $\pi\pi$ holes to be destabilized somewhat relative to the state with the $\delta\delta$ holes. However, there is an additional important effect here. At large R the separation between the $\pi\pi$ and $\delta\delta$ $^3\Sigma^-$ states is only 1.09 eV (a separation that would be expected to decrease as R decreases), and in the CI there is a strong interaction between these pure configurations leading to a major stabilization of the state with the $\pi\pi$ holes and destabilization of the state with the $\delta\delta$ holes. (This effect involves an interpair correlation which increases the average separation between the electrons in the doubly occupied δ^+ and δ^- orbitals.) The net result is that the state with the $\pi\pi$ hole ends up below the state with the $\delta\pi$ holes leading to the ordering

$$\delta\sigma < \pi\pi < \delta\pi < \sigma\pi < \delta\delta$$

In Table III we summarize the atomic and molecular configurations of the s^2d^8 states of NiCO. The energies are from an extensive CI calculation using 24 basis functions as described in section VI.

Table III. CI Energies for the s^2d^8 and s^1d^9 States of NiCO (R_{NiC} = 1.84 Å)

Holes	Atomic states	Atomic energy, eV[a]	Dominant molecular configuration										No.[b] conf	Mol state	Energy, eV
			O(2s)	C(2s)	3dσ	4s	σ	σ*	π_x	π_y	δ_{xy}	$\delta_{x^2-y^2}$			
							s^2d^8 states								
δδ	20% ^{3}F, 80% ^{3}P	1.49	2	2	2	2	2	0	2 2 0 0 0 0	2 2 0 0 0 0	1 0	1 0	1320	$2\,^3\Sigma^-$	5.290
σπ	40% ^{3}F, 60% ^{3}P	1.13	2	2	1	2	2	0	1 2 0 0 0 0	2 2 0 0 0 0	2 0	2 0	1192	$3\,^3\Pi$	4.390
δπ	100% ^{3}F	0.03	2	2	2	2	2	0	1 2 0 0 0 0	2 2 0 0 0 0	2 0	1 0	1320	$2\,^3\Pi$	3.988
			2	2	2	2	2	0	2 2 0 0 0 0	1 2 0 0 0 0	1 0	2 0		$^3\Phi^d$	3.034
ππ	80% ^{3}F, 20% ^{3}P	0.40	2	2	2	2	2	0	1 2 0 0 0 0	1 2 0 0 0 0	2 0	2 0	1320	$1\,^3\Sigma^-$	3.130
δσ	100% ^{3}F	0.03	2	2	1	2	2	0	2 2 0 0 0 0	2 2 0 0 0 0	1 0	2 0	1208	$2\,^3\Delta$	3.020
							s^1d^9 states								
π	100% ^{3}D	0.00	2	2	2	1	2	0	1 2 0 0 0 0	2 2 0 0 0 0	2 0	2 0	1192	$1\,^3\Pi$	0.400
σ	100% ^{3}D	0.00	2	2	1	1	2	0	2 2 0 0 0 0	2 2 0 0 0 0	2 0	2 0	698	$1\,^3\Sigma^+$	0.304
δ	100% ^{3}D	0.00	2	2	2	1	2	0	2 2 0 0 0 0	2 2 0 0 0 0	1 0	2 0	1208	$1\,^3\Delta$	0.000[c]

[a] Experimental numbers. [b] Number of spin eigenfunctions. [c] The total energy is −153.341 77. All other energies are relative to this energy. [d] $^3\Phi$ corresponds to (−) phase, whereas $^3\Pi$ corresponds to (+) phase.

Table IV. Generating Configurations for the $^3\Sigma^+$, $^3\Pi$, and $^3\Delta$ CI Calculations

State	Conf set	O(2s)	C(2s)	3dσ	4s	σ	σ*	π_x	π_y	δ_{xy}	$\delta_{x^2-y^2}$
$^3\Sigma^+$	A	2	2	1	1	2	0	2 2 0 0 0 0	2 2 0 0 0 0	2	2
		2	2	1	1	1	1	2 2 0 0 0 0	2 2 0 0 0 0	2	2
		2	2	1	1	2	0	2 1 1 0 0 0	2 2 0 0 0 0	2	2
		2	2	1	1	2	0	2 2 0 0 0 0	2 1 1 0 0 0	2	2
$^3\Delta$	A	2	2	2	1	2	0	2 2 0 0 0 0	2 2 0 0 0 0	1	2
		2	2	2	1	1	1	2 2 0 0 0 0	2 2 0 0 0 0	1	2
		2	2	2	1	2	0	2 1 1 0 0 0	2 2 0 0 0 0	1	2
		2	2	2	1	2	0	2 2 0 0 0 0	2 1 1 0 0 0	1	2
$^3\Delta$	B	2	2	1	2	2	0	2 2 0 0 0 0	2 2 0 0 0 0	1	2
		2	2	1	2	1	1	2 2 0 0 0 0	2 2 0 0 0 0	1	2
		2	2	1	2	2	0	2 1 1 0 0 0	2 2 0 0 0 0	1	2
		2	2	1	2	2	0	2 2 0 0 0 0	2 1 1 0 0 0	1	2
$^3\Pi$	A	2	2	2	1	2	0	1 2 0 0 0 0	2 2 0 0 0 0	2	2
		2	2	2	1	1	1	1 2 0 0 0 0	2 2 0 0 0 0	2	2
		2	2	2	1	2	0	1 1 1 0 0 0	2 2 0 0 0 0	2	2
		2	2	2	1	2	0	1 2 0 0 0 0	2 1 1 0 0 0	2	2
$^3\Pi$	B	2	2	1	2	2	0	1 2 0 0 0 0	2 2 0 0 0 0	2	2
		2	2	1	2	1	1	1 2 0 0 0 0	2 2 0 0 0 0	2	2
		2	2	1	2	2	0	1 1 1 0 0 0	2 2 0 0 0 0	2	2
		2	2	1	2	2	0	1 2 0 0 0 0	2 1 1 0 0 0	2	2

Of the states listed in Table III, the dipole-allowed transitions involving only a single one-electron transition (for the dominant configuration) are: $1\,^3\Delta \rightarrow 2\,^3\Delta$ ($3d\sigma \rightarrow 4s$) at 3.02 eV, $1\,^3\Delta \rightarrow {}^3\Phi$ ($3d\pi_x \rightarrow 4s$) at 3.03 eV, $1\,^3\Delta \rightarrow 2\,^3\Pi$ ($3d\pi_y \rightarrow 4s$) at 3.99 eV, $1\,^3\Sigma^+ \rightarrow 3\,^3\Pi$ ($3d\pi_x \rightarrow 4s$) at 4.09 eV, $1\,^3\Pi \rightarrow 1\,^3\Sigma^-$ ($3d\pi_y \rightarrow 4s$) at 2.73 eV, $1\,^3\Pi \rightarrow 3\,^3\Pi$ ($3d\sigma \rightarrow 4s$) at 3.99 eV, $1\,^3\Pi \rightarrow {}^3\Phi$ ($3d\delta_{x^2-y^2} \rightarrow 4s$) at 2.63 eV, and $1\,^3\Pi \rightarrow 2\,^3\Pi$ ($3d\delta_{x^2-y^2} \rightarrow 4s$) at 3.59 eV. All of these transitions involve 3d $\rightleftarrows$ 4s atomic transitions which are parity forbidden ($g \rightleftarrows g$) for the atom and consequently are not expected to be strong.

VI. The CI Calculations

A. The $^3\Sigma^+$, $^3\Pi$, $^3\Delta$ States. GVB-CI calculations were carried out for the $^3\Sigma^+$, $^3\Pi$, $^3\Delta$ states of NiCO using as a basis the self-consistent GVB orbitals for each state. Preliminary CI calculations including all single and double excitations from the dominant configuration for each state indicated that all the important configurations are obtained by allowing all single excitations from the A configurations in Table IV. In addition, for the $^3\Delta$ and $^3\Pi$ states we found that significant energy lowerings (~0.2 eV) resulted if the B configurations, which describe the $3\,^3\Pi$, $2\,^3\Delta$ states (of s^2d^8 character), were added to the list of generating configurations. (No comparable s^2d^8 state exists for the $^3\Sigma^+$ state.)

To allow for possible readjustment effects due to relaxation of the perfect pairing and strong orthogonality restrictions, the π space was augmented by adding three π virtuals in each direction chosen as the more diffuse atomic basis function of Ni(3dπ), C(2pπ), and O(2pπ) type, respectively (subsequently orthogonalized to the valence orbitals for the CI). The presence of these functions in the CI allows the π orbitals (in the CI) to change their radial extent on the three centers. The final CI included all single excitations from the A and B configurations in Table III into the full CI basis (20 functions after eliminating the C1s- and O1s-like functions by appropriate readjustment of the one-electron integrals). This CI thus includes the important configurations from the single and double excitation GVB-CI, the orbital readjustment effects within the full π space, and the effects from mixing in s^2d^8 character. This procedure resulted in 112, 180, and 172 spatial configurations (538, 852, 988 spin eigenfunctions; 833, 1312, 1564 determinants) for the $^3\Sigma^+$, $^3\Pi$, and $^3\Delta$ states, respectively.

In order to determine the relative importance of each configuration in the CI, the energy lowering is computed according to the formula

Table V. Energy Contribution of Dominant Configurations[a] of the GVB–CI Wave Functions for the $^3\Sigma^+$, $^3\Pi$, and $^3\Delta$ States of NiCO (R_{NiC} = 1.84 Å)

State	No.	Character[b]	Configuration										Energy contribution, mh[c]
			O(2s)	C(2s)	3dσ	4s	σ	σ*	π_x	π_y	δ_{xy}	$\delta_{x^2-y^2}$	
$^3\Sigma^+$	1	HF	2	2	1	1	2	0	220000	220000	2	2	
	2	I(π_x, π_y)	2	2	1	1	2	0	211000	211000	2	2	17.8
	3	C(π_x)	2	2	1	1	2	0	202000	220000	2	2	14.5
	4	C(π_y)	2	2	1	1	2	0	220000	202000	2	2	14.5
	5	I(σ, π_y)	2	2	1	1	1	1	220000	211000	2	2	12.2
	6	I(σ, π_x)	2	2	1	1	1	1	211000	220000	2	2	12.2
	7	C(σ)	2	2	1	1	0	2	220000	220000	2	2	7.5
$^3\Pi$	1	HF	2	2	2	1	2	0	120000	220000	2	2	
	2	I(π_x, π_y)	2	2	2	1	2	0	111000	211000	2	2	17.9
	3	C(π_x)	2	2	2	1	2	0	102000	220000	2	2	15.1
	4	C(π_y)	2	2	2	1	2	0	120000	202000	2	2	14.3
	5	I(σ, π_x)	2	2	2	1	1	1	110000	220000	2	2	12.3
	6	I(σ, π_y)	2	2	2	1	1	1	120000	211000	2	2	12.1
	7	C(σ)	2	2	2	1	0	2	120000	220000	2	2	7.4
	8	R($1\pi_x$, $2\pi_x$)	2	2	2	1	2	0	210000	220000	2	2	2.2
	9	M, R($1\pi_y$, $4\pi_y$)	2	2	1	2	2	0	120000	120100	2	2	1.0
$^3\Delta$	1	HF	2	2	2	1	2	0	220000	220000	1	2	
	2	I(π_x, π_y)	2	2	2	1	2	0	211000	211000	1	2	18.3
	3	C(π_x)	2	2	2	1	2	0	202000	220000	1	2	14.4
	4	C(π_y)	2	2	2	1	2	0	220000	202000	1	2	14.4
	5	I(σ, π_y)	2	2	2	1	1	1	220000	211000	1	2	12.3
	6	I(σ, π_x)	2	2	2	1	1	1	211000	220000	1	2	12.3
	7	C(σ)	2	2	2	1	0	2	220000	220000	1	2	7.4
	8	M	2	2	1	2	2	0	220000	220000	1	2	2.5
	9	M, R($1\pi_x$, $4\pi_x$)	2	2	1	2	2	0	120100	220000	1	2	1.7
	10	M, R($1\pi_y$, $4\pi_y$)	2	2	1	2	2	0	220000	120100	1	2	1.7

[a] All configurations contributing 1 mhartree or more are listed. [b] R indicates an orbital readjustment effect (single excitation); C indicates correlation of a particular doubly occupied orbital; I indicates an interpair correlation effect; M indicates mixing in of s^2d^8 character. [c] 1 mhartree = 10^{-3} hartree = 0.027 eV.

Table VI. Energy Contribution of the Dominant Configuration of the GVB–CI Wave Function for the X $^1\Sigma_g^+$ State of CO

No.	Character[a]	Configuration						Energy contribution, mhartrees
		O(2s)	C(2s)	σ	σ*	π_x	π_y	
1	HF	2	2	2	0	2000	2000	
2	I(π_x, π_y)	2	2	2	0	1100	1100	21.4
3	C(π_x)	2	2	2	0	0200	2000	13.9
4	C(π_y)	2	2	2	0	2000	0200	13.9
5	I(σ, π_x)	2	2	1	1	1100	2000	13.8
6	I(σ, π_y)	2	2	1	1	2000	1100	13.8
7	C(σ)	2	2	0	2	2000	2000	7.2

[a] The same notation as Table V is used here.

Table VII. Energies for the $^3\Sigma^+$, $^3\Pi$, and $^3\Delta$ States of NiCO[a]

		$R = 3.20a_0$ (1.69 Å)	$R = 3.48a_0$ (1.84 Å)	$R = 3.80a_0$ (2.01 Å)
$^3\Sigma^+$	GVB	−153.258 51	−153.271 61	−153.272 82
	CI	−153.318 77	−153.331 48	−153.332 48
$^3\Delta$	GVB	−153.262 19	−153.272 29	−153.271 12
	CI	−153.326 77	−153.336 16	−153.334 20
$^3\Pi$	GVB	−153.239 69	−153.258 36	−153.263 55
	CI	−153.302 94	−153.320 49	−153.324 71

[a] At $R = \infty$ the energies for Ni(^{3}D) + CO X $^1\Sigma_g^+$ are −153.243 11 and −153.300 56 hartrees for the GVB and CI wave functions, respectively.

Table VIII. Potential Curve Parameters from the CI Calculations on NiCO

	R_e, Å	D_e, eV[a]	ω_e, cm^{-1}
$^3\Delta$	1.901	1.145	427.5
$^3\Sigma^+$	1.937	0.905	441.3
$^3\Pi$	1.968	0.852	477.5

[a] We have included in D_e the additional energy lowering obtained in the 24 basis function CI at R = 1.84 Å. With the 20 basis function CI for each R, we obtained D_e of 0.992, 0.905, and 0.671 eV for these states.

$$\Delta E_\mu = C_\mu^2(E - H_{\mu\mu})/(1 - C_\mu^2) \qquad (16)$$

This is the energy increase that would result if configuration μ were deleted while keeping all other CI coefficients fixed. In cases where there is more than one spin eigenfunction for a given spatial configuration, we have simply added the separate contributions due to each spin eigenfunction. The ΔE_μ provides an indication of the relative importance of configurations, although the sum of the ΔE_μ does not equal the total energy lowering.

Table V shows the dominant configurations in the CI wave

Table IX. Generating Configurations for the 24 Basis Function CI

State	O(2s)	C2(s)	3dσ	4s	σ	σ*	3dσ′	4s′	π_x	π_y	δ_{xy}	$\delta_{x^2-y^2}$
$^3\Sigma^+$	2	2	1	1	2	0	0	0	220000	220000	20	20
	2	2	1	1	1	1	0	0	220000	220000	20	20
	2	2	1	1	2	0	0	0	211000	220000	20	20
	2	2	1	1	2	0	0	0	220000	211000	20	20
$^3\Phi^a$	2	2	2	2	2	0	0	0	120000	220000	20	10
	2	2	2	2	1	1	0	0	120000	220000	20	10
	2	2	2	2	2	0	0	0	111000	220000	20	10
	2	2	2	2	2	0	0	0	120000	211000	20	10
	2	2	2	2	2	0	0	0	220000	120000	10	20
	2	2	2	2	1		0	0	220000	120000	10	20
	2	2	2	2	2	0	0	0	220000	111000	10	20
	2	2	2	2	2	0	0	0	211000	120000	10	20
$^3\Pi$	2	2	2	1	2	0	0	0	120000	220000	20	20
	2	2	2	1	1	1	0	0	120000	220000	20	20
	2	2	2	1	2	0	0	0	111000	220000	20	20
	2	2	2	1	2	0	0	0	120000	211000	20	20
	2	2	1	2	2	0	0	0	120000	220000	20	20
	2	2	1	2	1	1	0	0	120000	220000	20	20
	2	2	1	2	2	0	0	0	111000	220000	20	20
	2	2	1	2	2	0	0	0	120000	211000	20	20
$^3\Sigma^-$	2	2	2	2	2	0	0	0	120000	120000	20	20
	2	2	2	2	1	1	0	0	120000	120000	20	20
	2	2	2	2	2	0	0	0	111000	120000	20	20
	2	2	2	2	2	0	0	0	120000	111000	20	20
	2	2	2	2	2	0	0	0	220000	220000	10	10
	2	2	2	2	1	1	0	0	220000	220000	10	10
	2	2	2	2	2	0	0	0	211000	220000	10	10
	2	2	2	2	2	0	0	0	220000	211000	10	10
$^3\Delta$	2	2	2	1	2	0	0	0	220000	220000	10	20
	2	2	2	1	1	1	0	0	220000	220000	10	20
	2	2	2	1	2	0	0	0	211000	220000	10	20
	2	2	2	1	2	0	0	0	220000	211000	10	20
	2	2	1	2	2	0	0	0	220000	220000	10	20
	2	2	1	2	1	1	0	0	220000	220000	10	20
	2	2	1	2	2	0	0	0	211000	220000	10	20
	2	2	1	2	2	0	0	0	220000	211000	10	20

[a] This group of configurations leads to both $^3\Phi$ and $^3\Pi$ states. Thus these configurations should be combined with the $^3\Pi$ configurations, leading to 2512 spin eigenfunctions. However, the 1 $^3\Pi$ and 3 $^3\Pi$ states are well described by excitations from the configurations listed under $^3\Pi$ while the 2 $^3\Pi$ state is well described by excitations from the configurations listed under $^3\Phi$. Hence we calculated these states separately, leading to slight errors for the 2 $^3\Pi$ and 3 $^3\Pi$ energies.

functions for the $^3\Sigma^+$, $^3\Pi$, $^3\Delta$ states of NiCO (at R = 1.84 Å). Table VI gives the same information for a comparable CI on CO. The configurations are characterized according to the notation explained in footnote *b* of Table IV. In general the three states of NiCO show correlation effects very similar to those seen in CO, but the $^3\Pi$ and $^3\Delta$ states show some mixing in of s^2d^8 character from the higher s^2d^8 state. The energies for the GVB and CI wave functions of the three states as a function of NiC separation are given in Table VII. For each state a parabola was fit through the three points to obtain the D_e, R_e, and ω_e values given in Table VIII.[20]

B. The s^2d^8 States. A procedure for generating configurations similar to that used for the s^1d^9 states was used. The generating configurations are given in Table IX. As a CI basis the GVB orbitals of the $^3\Delta$ state (s^1d^9) were used. In order to describe readjustment effects, the π space was augmented as previously described for the s^1d^9 states and, in addition, functions were added which correspond to the more diffuse component of the $3d\delta_{xy}$, $3d\delta_{x^2-y^2}$, and $3d\sigma$ atomic orbitals. To describe the contraction of the 4s orbital appropriate to a $(4s)^2$ state the 4s orbital from an SCF calculation on the $^3\Phi$ state ($\delta\pi$ holes) was added as a virtual orbital. The resulting basis consisted of 24 functions.

All singles from the generating configurations in Table IX were included in the CI (with the restriction that excitations into the $3d\delta$ and 4s virtuals were allowed only for configurations of s^2 character and only from the 4s, $3d\sigma$, and C(2s)-like orbitals which would be expected to change in character for s^2 states). This leads to 144, 236, 236, 236, and 212 spatial configurations (698, 1320, 1192, 1320, and 1208 spin eigenfunctions; 1081, 2082, 1854, 2082, and 1910 determinants) for the $^3\Sigma^+$, $^3\Phi$, $^3\Pi$, $^3\Sigma^-$, and $^3\Delta$ CI's, respectively.

The CI energies have been presented in Table III. In Table X we show the dominant configurations and energy lowerings for each of the states. For the s^1d^9 states the energy contributions for each important configuration are generally the same as for the smaller 20 basis function CI (used to derive the properties of the potential curves). A notable exception is for the 1 $^3\Delta$ state where configuration 5 (which describes mixing in of s^2d^8 character) contributes 11.9 mhartrees for the larger CI, whereas it contributed only 2.5 mhartrees in the smaller CI. This effect is due to a better description of the 2 $^3\Delta$ state which lowers this state by 1.21 eV relative to the 20 basis function CI; as a result there is greater interaction with the 1 $^3\Delta$ state, leading to an additional energy lowering of 0.153 eV. Adding this lowering (at 1.84 Å) to the D_e obtained with the smaller CI at the optimum R (R_e = 1.90 Å) leads to 1.145 eV as our best estimate of D_e for the $^3\Delta$ state.

Table X. Energy Contributions of the Dominant Configurations ($\Delta E > 10$ mhartree) for each of the Roots of the 24 Basis Function CI[a]

State	No.	Character	Configuration												Energy contribn mhartrees
			O(2s)	C(2s)	3dα	4s	σ	σ*	3dσ′	4s′	π_x	π_y	δ_y	$\delta_{x^2-y^2}$	
$1\,^3\Delta$	1	HF	2	2	2	1	2	0	0	0	220000	220000	10	20	
	2	I($2\pi_x$, $2\pi_y$)	2	2	2	1	2	0	0	0	211000	211000	10	20	17.7
	3	C($2\pi_x$)	2	2	2	1	2	0	0	0	202000	220000	10	20	13.9
	4	C($2\pi_y$)	2	2	2	1	2	0	0	0	220000	202000	10	20	13.9
	5	M	2	2	1	2	2	0	0	0	220000	220000	10	20	11.9
$2\,^3\Delta$	1	HF	2	2	1	2	2	0	0	0	220000	220000	10	20	
	2	I($2\pi_x$, $2\pi_y$)	2	2	1	2	2	0	0	0	211000	211000	10	20	17.0
	3	R(4s)	2	2	1	1	2	0	0	1	220000	220000	10	20	13.4
	4	C($2\pi_y$)	2	2	1	2	2	0	0	0	220000	202000	10	20	12.8
	5	C($2\pi_x$)	2	2	1	2	2	0	0	0	202000	220000	10	20	12.8
	6	R($1\pi_y$)	2	2	1	2	2	0	0	0	220000	121010	10	20	12.2
	7	R($1\pi_x$)	2	2	1	2	2	0	0	0	121010	220000	10	20	12.2
	8	I(σ, $2\pi_y$)	2	2	1	2	1	1	0	0	220000	211000	10	20	10.9
	9	I(σ, $2\pi_x$)	2	2	1	2	1	1	0	0	211000	22000	10	20	10.9
$^3\Sigma^+$	1	HF	2	2	1	1	2	0	0	0	220000	220000	20	20	
	2	R(C(2s), 3dσ)	2	1	2	1	2	0	0	0	220000	220000	20	20	17.5
	3	I($2\pi_x$, $2\pi_y$)	2	2	1	1	2	0	0	0	211000	211000	20	20	16.9
	4	C($2\pi_y$)	2	2	1	1	2	0	0	0	220000	202000	20	20	13.7
	5	C($2\pi_x$)	2	2	1	1	2	0	0	0	202000	220000	20	20	13.7
	6	I(σ, $2\pi_y$)	2	2	1	1	1	1	0	0	220000	211000	20	20	11.7
	7	I(σ, $2\pi_x$)	2	2	1	1	1	1	0	0	211000	220000	20	20	11.7
$1\,^3\Pi$	1	HF	2	2	2	1	2	0	0	0	120000	220000	20	20	
	2	I($2\pi_x$, $2\pi_y$)	2	2	2	1	2	0	0	0	111000	211000	20	20	17.5
	3	C($2\pi_x$)	2	2	2	1	2	0	0	0	102000	220000	20	20	14.8
	4	C($2\pi_y$)	2	2	2	1	2	0	0	0	120000	202000	20	20	13.9
	5	I(σ, $2\pi_x$)	2	2	2	1	1	1	0	0	111000	220000	20	20	12.0
	6	I(σ, $2\pi_y$)	2	2	2	1	1	1	0	0	120000	211000	20	20	11.7
$3\,^3\Pi$	1	HF	2	2	1	2	2	0	0	0	120000	220000	20	20	
	2	I($2\pi_x$, $2\pi_y$)	2	2	1	2	2	0	0	0	111000	211000	20	20	16.8
	3	R(4s)	2	2	1	1	2	0	0	1	120000	220000	20	20	14.9
	4	C($2\pi_x$)	2	2	1	2	2	0	0	0	102000	220000	20	20	13.4
	5	C($2\pi_y$)	2	2	1	2	2	0	0	0	120000	202000	20	20	13.2
	6	R($1\pi_y$)	2	2	1	2	2	0	0	0	120000	120100	20	20	11.8
	7	R(3dσ)	2	2	0	2	2	0	1	0	120000	220000	20	20	11.0
	8	I(σ, $2\pi_x$)	2	2	1	2	1	1	0	0	111000	220000	20	20	11.0
	9	I(σ, $2\pi_y$)	2	2	1	2	1	1	0	0	120000	211000	20	20	11.0
	10	R($2\pi_x$)	2	2	1	2	2	0	0	0	201000	220000	20	20	10.2
$1\,^3\Sigma^-$	1	HF	2	2	2	2	2	0	0	0	120000	120000	20	20	
	2	I(π, δ)	2	2	2	2	2	0	0	0	220000	220000	10	10	99.8
	3	R(3dσ)	2	2	1	2	2	0	1	0	120000	120000	20	20	15.1
	4	I($2\pi_x$, $2\pi_y$)	2	2	2	2	2	0	0	0	111000	111000	20	20	13.1
	5	R(4s)	2	2	2	1	2	0	0	1	120000	120000	20	20	12.7
$2\,^3\Sigma^-$	1	HF	2	2	2	2	2	0	0	0	220000	220000	10	10	
	2	I(π, δ)	2	2	2	2	2	0	0	0	120000	120000	20	20	61.4
	3	I($2\pi_x$, $2\pi_y$)	2	2	2	2	2	0	0	0	211000	211000	10	10	15.4
	4	R($1\pi_y$)	2	2	2	2	2	0	0	0	220000	120100	10	10	12.2
	5	R($1\pi_x$)	2	2	2	2	2	0	0	0	120100	220000	10	10	12.2
	6	R(4s)	2	2	2	1	2	0	0	1	220000	220000	10	10	10.5
	7	R(3dσ)	2	2	1	2	2	0	1	0	220000	220000	10	10	10.2
$^3\Phi$	1	HF	2	2	2	2	2	0	0	0	220000	120000	10	20	[b]
	2	HF	2	2	2	2	2	0	0	0	120000	220000	20	10	
$2\,^3\Pi$	1	HF	2	2	2	2	2	0	0	0	220000	120000	10	20	[c]
	2	HF	2	2	2	2	2	0	0	0	120000	220000	20	10	

[a] The notation for describing the character of each configuration is the same as for Tables V and VI. [b] The coefficients are equal in magnitude but opposite in phase. [c] The coefficients are of the same magnitude and phase.

VII. Comparison of Results with the MEP and AIEP

In Table XI we show the GVB bond energies for selected states of NiCO for which calculations using the AIEP are available. The results from the AIEP are expected to be quite close (within 0.2 eV) to what would be obtained from corresponding ab initio calculations. Here we see that at $R = 1.84$ Å the best state ($2\,^3\Delta$) has $(4s)^2(3d)^8$ character and is 2.2 eV *above* the energy for ground state atoms. Thus we obtain the wrong character and no bond. The $^3\Sigma^+$ state has $(4s)^1(3d)^9$ character and one might argue that its energy should be compared with that of the corresponding atomic state (since the ab initio HF wave function discriminates against this state by 2.3 eV). However, even in this case the calculated bond energy is negative although only by 0.2 eV.

The problem here is clearly related to the fact that the AIEP (in conjunction with the usual basis set) leads to an incorrect bias toward s^2d^8 states for the Ni atom. Thus for molecular

Table XI. Bond Energies at R_{NiC} = 1.84 Å from GVB(3) Calculations on Selected States of NiCO Using the AIEP

Dominant configuration										Corresponding State using the MEP	Bond energy, eV rel to	
O(2s)	C(2s)	3dσ	4s	σ	σ*	π_x	π_y	δ_{xy}	$\delta_{x^2-y^2}$		^{3}D	^{3}F
2	2	1	2	2	0	2 2 0	2 2 0	1	2	$2\,^3\Delta$	+0.11	−2.18
2	2	1	1	2	0	2 2 0	2 2 0	2	2	$^3\Sigma^+$	−0.17	−2.47
2	2	2	2	2	0	1 2 0	2 2 0	1	2	$^3\Phi$	−1.21	−3.50

systems there is a comparable bias toward s^2d^8 states which are unfavorable for bonding in NiCO. One might hope to correct this error by adding additional s, p, d, and f basis functions on the Ni and including the appropriate correlation effects; however, to carry out a comparable CI would involve an enormously increased number of configurations. At the present time such calculations of potential curves for numerous excited states are not practical and we conclude that use of the MEP, which *does* lead to reasonable results, is a better alternative.

VIII. Summary

Since the 4s orbital has a significant overlap with the CO lone pair, the $(4s)^2$ state of Ni leads to strong repulsive interaction when the CO is pushed close enough to overlap the d orbitals of the Ni. As a result, the three bound states of NiCO all have s^1d^9 character on the Ni. We find similar results for bonding of CO to two and three Ni and expect these conclusions to apply also to CO bonded to the Ni surface.

Of the three bound states a strong intraatomic coupling effect leads to stabilization of the $^3\Delta$ state (δ hole) over the $^3\Sigma^+$ (σ hole) and $^3\Pi$ (π hole) states. The $^3\Delta$ and $^3\Sigma^+$ states exhibit greater π back-bonding than $^3\Pi$ and consequently lie lower. The resulting bond energies are 1.15 eV ($^3\Delta$), 0.91 eV ($^3\Sigma^+$), and 0.85 eV ($^3\Pi$). The optimum NiC bond length ($^3\Delta$) is found to be 1.90 Å which is slightly longer than that of $Ni(CO)_4$, 1.84 Å. The vibrational frequency is calculated at 428 cm^{-1}.

Ab initio HF calculations (using the usual basis set) on the states of Ni put the $^3D(s^1d^9)$ state 2.3 eV above the $^3F(s^2d^8)$ state, whereas experimentally these states are essentially degenerate. In order to obtain the correct atomic separations, additional basis functions and correlation effects must be included, a procedure which is not practical for molecules. Use of the ab initio effective potential (AIEP) should yield results in close agreement (errors <0.2 eV) with the ab initio results. However, because the bonding in NiCO involves the $^3D(s^1d^9)$ state, which is very poorly described with the AIEP, use of the AIEP for NiCO leads to no bond whatsoever. In the calculations reported here we have used a modified effective potential (MEP) which is adjusted so as to yield the correct separation of the atomic states while not modifying the sizes of the orbitals. The results obtained for NiCO with the MEP are in agreement with the fragmentary experimental information available and provide evidence for the efficacy of this approach.

References and Notes

(1) Supported by a grant (DMR74-04965) from the National Science Foundation with some support from a grant (PRF No. 7683-AC6) from the donors of the Petroleum Research Fund, administered by the American Chemical Society.
(2) Partially supported by a grant (CHE73-05132) from the National Science Foundation.
(3) R. L. De Kock, *Inorg. Chem.*, **10**, 1205 (1971).
(4) W. A. Goddard III, T. H. Dunning, Jr., W. J. Hunt, and P. J. Hay, *Acc. Chem. Res.*, **6**, 368 (1973).
(5) C. F. Melius, B. D. Olafson, and W. A. Goddard III, *Chem. Phys. Lett.*, **28**, 457 (1974); C. F. Melius and W. A. Goddard III, *Phys. Rev. A*, **10**, 1528 (1974).
(6) The quoted atomic separations are obtained by taking a weighted average over the spectral levels corresponding to a given L and S (spin–orbit interactions are not included in our calculation). The values are from ref 7.
(7) C. E. Moore, "Atomic Energy Levels", Vol. II, National Bureau of Standards, 1952.
(8) M. J. Sollenberger, W. A. Goddard III, and C. F. Melius, manuscript to be submitted.
(9) A. J. H. Wachters, *J. Chem. Phys.*, **52**, 1033 (1970).
(10) T. H. Dunning, Jr., unpublished work. The p functions are the same as in ref 11, the tightest seven s basis functions are contracted into a single basis function based on the 1s HF orbital, the second and third most diffuse are contracted into a basis function based on the 2s HF orbital; the most diffuse function is uncontracted.
(11) T. H. Dunning, Jr., *J. Chem. Phys.*, **53**, 2823 (1970).
(12) F. A. Cotton and G. Wilkinson, "Advanced Inorganic Chemistry", 3rd ed, Interscience, New York, N.Y., 1972, p 684.
(13) See ref 3 and references cited therein.
(14) L. B. Harding and W. A. Goddard III, *J. Am. Chem. Soc.*, **97**, 6293 (1975).
(15) The second natural orbital of each π pair is similar to the orbital that would be used to correlate angularly the C(2s) pair. Thus, since all of the natural orbitals must be orthogonal in a GVB–PP calculation, we cannot simultaneously obtain optimal correlation of the C(2s) and π pairs in a given direction. Since the π pair leads to a larger energy lowering, a better energy is obtained by correlating both π pairs. In a CI calculation over these orbitals, configurations can be included that describe simultaneous correlation of the C(2s) and π pairs.
(16) The percentage of ^{3}P and ^{3}F corresponding to each determinant was determined in a manner analogous to the derivation of eq 14 in section IV.C.
(17) The analysis of this section is based on the analysis by C. F. Melius and W. A. Goddard III of the states of NiH and Ni_2.
(18) In (12) [CORE] is different from (11) since [CORE] includes all the doubly occupied orbitals.
(19) Again, [CORE] contains all doubly occupied dπ and dδ orbitals.
(20) The energy of the separated limits was taken as the Ni(^{3}D) HF energy plus the energy for a comparable CI on CO. At $R = \infty$ the procedure for selecting configurations results in only single excitations involving the Ni; thus the CI leads to just the HF wave function for the Ni atom.
(21) T. Smedley and W. A. Goddard III, unpublished calculations.